33. Toma JG, et al. Isolation of multipotent adult stem cells from the dermis of mammalian skin. *Nat Cell Biol.* 2001;3(9):778–784.
34. Akiyama H, et al. Interactions between Sox9 and beta-catenin control chondrocyte differentiation. *Genes Dev.* 2004;18(9):1072–1087.
35. Koelling S, et al. Migratory chondrogenic progenitor cells from repair tissue during the later stages of human osteoarthritis. *Cell Stem Cell.* 2009; 4(4):324–335.
36. Nagy A, Gertsenstein M, Vintersten K, Behringer R. *Manipulating the Mouse Embryo.* New York, New York, USA: Cold Spring Harbor Laboratory Press; 2003.
37. Bjorntorp P, Karlsson M, Pertoft H, Pettersson P, Sjostrom L, Smith U. Isolation and characterization of cells from rat adipose tissue developing into adipocytes. *J Lipid Res.* 1978;19(3):316–324.
38. Lefebvre V, Garofalo S, Zhou G, Metsaranta M, Vuorio E, De Crombrugghe B. Characterization of primary cultures of chondrocytes from type II collagen/beta-galactosidase transgenic mice. *Matrix Biol.* 1994;14(4):329–335.
39. Aszodi A, Hunziker EB, Brakebusch C, Fassler R. Beta1 integrins regulate chondrocyte rotation, G1 progression, and cytokinesis. *Genes Dev.* 2003;17(19):2465–2479.
40. Kitamura T, et al. Retrovirus-mediated gene transfer and expression cloning: powerful tools in functional genomics. *Exp Hematol.* 2003; 31(11):1007–1014.

THE JOURNAL OF
Obstetrics and Gynaecology Research

The official Journal of Asia and Oceania Federation of Obstetrics and Gynaecology
Japan Society of Obstetrics and Gynecology

doi:10.1111/j.1447-0756.2010.01324.x

J. Obstet. Gynaecol. Res. 2010

Prenatal diagnosis of short-rib polydactyly syndrome type 3 (Verma-Naumoff type) by three-dimensional helical computed tomography

Takahiro Yamada[1], Gen Nishimura[2], Keiichiro Nishida[3], Hideaki Sawai[4], Tokuhiko Omatsu[5], Taichi Kimura[6], Hiroshi Nishihara[6], Rina Shono[1], Shigeki Shimada[1], Mamoru Morikawa[1], Masato Mizushima[1], Takashi Yamada[1], Kazutoshi Cho[1], Shinya Tanaka[6], Hiroki Shirato[5] and Hisanori Minakami[1]

Departments of [1]Obstetrics and Gynecology, [5]Radiology, and [6]Molecular and Cellular Pathology, Hokkaido University Graduate School of Medicine, Sapporo, [2]Department of Radiology, Tokyo Metropolitan Kiyose Children's Hospital, Kiyose, [3]Department of Human Morphology, Okayama University Graduate School of Medicine and Dentistry, Okayama, and [4]Department of Obstetrics and Gynecology, Hyogo College of Medicine, Nishinomiya, Japan

Abstract

We present a case of short-rib polydactyly syndrome (SRPs) type 3 in which accurate prenatal diagnosis was feasible using both ultrasonography and 3D-CT. SRP encompass a heterogeneous group of lethal skeletal dysplasias. However, the phenotypes overlap with those of nonlethal skeletal dysplasias (i.e. Ellis-van Creveld syndrome and Jeune syndrome). As accurate prenatal diagnosis of SRP is helpful for parents, we used 3D-CT in the early third trimester to examine a fetus suggested to have phenotypes of 'short-rib dysplasia group' on ultrasonography. 3D-CT showed mild modification of the vertebral bodies, small ilia with horizontal acetabula and triangular partial ossification defects, and subtle metaphyseal irregularities of the femora. These CT findings and an extensive literature search regarding the phenotypes of various diseases categorized as short-rib dysplasia group led to a correct prenatal diagnosis of SRP type 3. This case exemplified the usefulness of 3D-CT for the precise prenatal diagnosis of skeletal dysplasias.

Key words: 3D-CT, asphyxiating thoracic dystrophy, Jeune syndrome, prenatal diagnosis, short-rib polydactyly syndrome.

Introduction

Short-rib polydactyly syndromes (SRPs) encompass a heterogeneous group of lethal skeletal dysplasias that are inherited in an autosomal recessive manner. SRPs are classified into four types: type 1 (Saldino-Noonan; OMIM 263530), type 2 (Majewski; OMIM 263520), type 3 (Verma-Naumoff; OMIM 263510), and type 4 (Beemer-Langer; OMIM 269860). Nosology and Classification of Genetic Skeletal Disorders: 2006 Revision lists these disorders as 'short-rib dysplasia (with or without polydactyly) group'.[1] The constellation of a severely narrow thorax, short limbs, and polydactyly allows prenatal diagnosis of SRPs with fetal ultrasonography. However, the phenotypes of SRPs overlap with those of nonlethal, but occasionally semilethal, skeletal dysplasias that belong to the short-rib dysplasia group (i.e. Ellis-van Creveld syndrome [EvC]; OMIM 225500]) and asphyxiating thoracic dystrophy ([ATD] Jeune syndrome; OMIM 208500). Recent reports have suggested the usefulness of three-dimensional helical computed tomography (3D-CT) in the differential diagnosis of skeletal disorders.[2] Here, we report a fetus with SRP type 3 diagnosed prenatally

Received: August 10 2009.
Accepted: February 5 2010.
Reprint request to: Dr Takahiro Yamada, Department of Obstetrics and Gynecology, Hokkaido University Graduate School of Medicine, N15W7 Kita-ku, Sapporo 060-8638, Japan. Email: taka0197@med.hokudai.ac.jp

Table 1 Differential diagnosis and comparison between results of ultrasound, three-dimensional computed tomography (3D-CT), and postnatal examination of the fetus in the present case

	Present case				SRP1	SRP3	SRP2/4	ATD	EvCD
	Prenatal		Postnatal						
	Ultrasonography	3D-CT	Radiograph	Phenotype					
Head and face									
Macrocephaly	++	++	++	++	+	+	+	−	−
CNS abnormalities	−	NA	NA	−	+	+	+	−	+
Cleft lip	−	NA	NA	−	−	−	++	−	+
Shortened frenula	Unclear	NA	NA	++	++	++	++	−	+
High clavicles	Unclear	++	++	++	++	++	++	++	++
Bones									
Short limb	++	++	++	++	++	++	+	+	+
Polydactyly	++	++	++	++	++	++	++	+	++
Narrow thorax with short rib	++	++	++	++	++	++	++	+	+
Hypoplasia of tibia	−	−	−	−	−	−	++	−	−
Flaring of the metaphyses	+	++	++	++	−	++	−	−	−
Irregularity of the metaphyses	Unclear	+	+	+	+	+	−	+	−
Pointed metaphyses	Unclear	−	−	−	++	−	−	−	−
Spondylar dysplasia	Unclear	+	+	+	+	+	−	+	−
Hypoplasia of iliac bones	Unclear	++	++	++	++	++	−	++	++
Other organs									
Congenital heart defect	−	NA	NA	−	+	+	−	−	++
Renal abnormalities	−	NA	NA	+	+	+	+	+	−
Genital abnormalities	++	NA	NA	++	++	++	+	−	−

++, prominent; +, present; −, absent. CNS, central nervous system; NA, not applicable. This table is made based on findings of previous reports.[3,4,10,11]

based on fetal ultrasonography and additional 3D-CT. The present case represents another example indicating the powerful capability of 3D-CT in the prenatal diagnosis of fetal skeletal dysplasias.

Case Report

A 23-year-old primigravida was referred for further investigation of fetal short limbs at 28 weeks of gestation. She was in a non-consanguineous marriage and had neither relevant medical history nor significant family history. Ultrasonography of the fetus revealed a narrow and small thorax covering only the dorsal part of the viscera, short femora of 30 mm (−7.26 SD), short humeri of 29 mm (−6.27 SD), mild ulnar deviation of the hands, short digits, bilateral postaxial polydactyly in the hands and feet, and long biparietal diameter (BPD) of 79.0 mm (+2.7 SD) suggestive of macrocephaly. Bilateral renal dysplasia and penile hypoplasia were also suspected. The volume of amniotic fluid was normal. These findings suggested a lethal or semilethal skeletal dysplasia classified as belonging to the short-rib dysplasia group shown in Table 1. After obtaining informed consent, computed tomography (CT) was performed at 33 weeks of gestation with a 64-detector row CT scanner (Aquilion64; Toshiba Medical Systems, Tokyo, Japan) with the following parameters: collimation, 0.5 mm; peak tube potential, 100 kVP; gantry rotation time, 0.75 s; beam pitch, 53; and tube current between 260 and 335 mA using an automatic tube current modulation technique. The volume CT dose index (CTDIvol.) was 21.5 mGy. The data from the CT scanner were stored and transferred onto a workstation (ZIOSTATION; Ziosoft, Tokyo, Japan). Multiplanar reconstruction (MPR) and 3D reconstruction by shaded surface display (SSD) images of fetal bones were created and reviewed interactively on the workstation. They provided additional information, including high-rising clavicles, mild modification of the vertebral bodies, subtle metaphyseal irregularities of

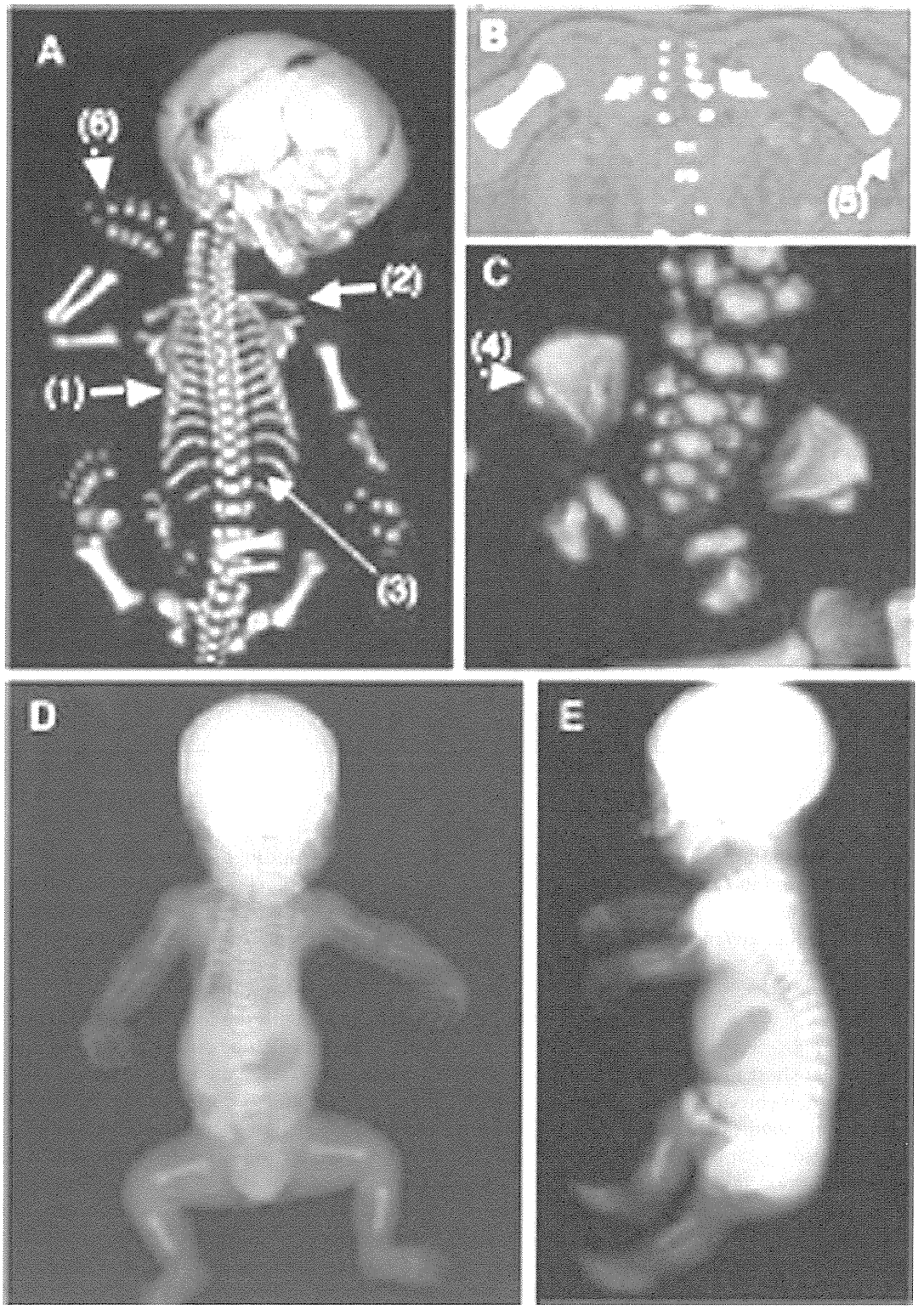

Figure 1 (a–c) Fetal computed tomography (CT) showed a narrow thorax (1), high-rising clavicles (2), mild modification of the vertebral bodies (3), small ilia with horizontal acetabula and triangular ossification defects at the inferior aspect of the lateral iliac margin (4), subtle metaphyseal irregularities of the femora (5), and brachydactyly with postaxial polydactyly (6). (d,e) Radiological findings on postnatal radiographs were identical to those of fetal CT.

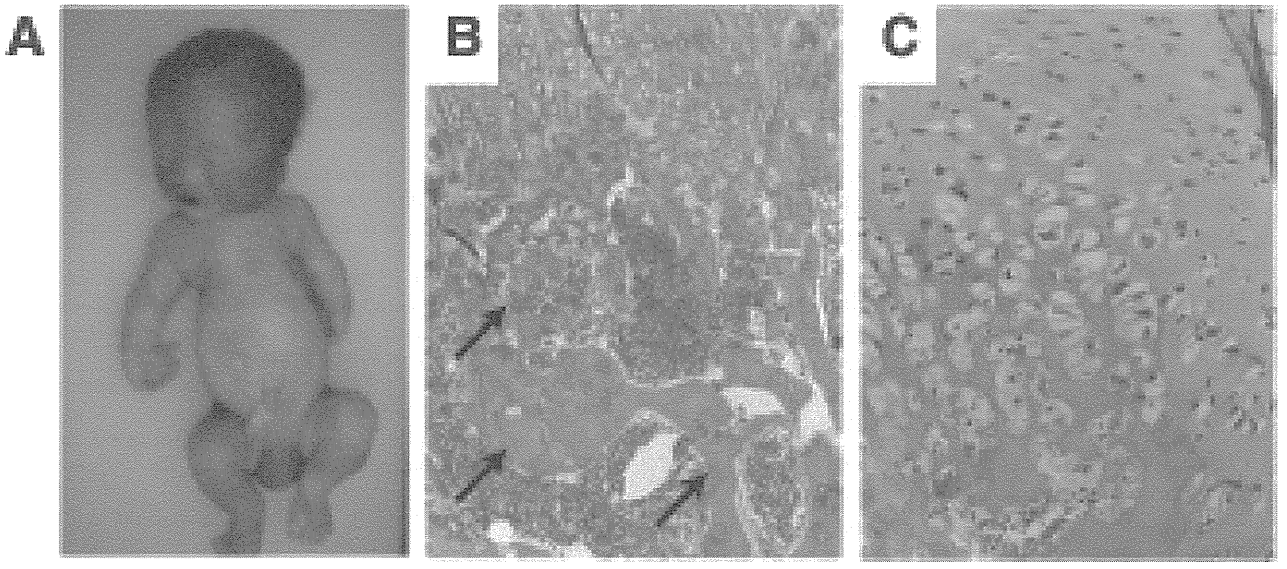

Figure 2 (a) Macroscopic view of the infant. The infant had macrocephaly, shortened frenula, club hands, polydactyly in the bilateral hands and feet, a bell-shaped narrow thorax, protruding abdomen, hypoplasia of the bilateral kidneys, bilateral dilated ureter, hydropic scrotum, and absent penis. (b,c) Histological findings of growth plate cartilage at costochondral junction. (b) There was loss of columnization with irregularly dispersed hypertrophic cells. The numbers of resting and hypertrophic chondrocytes were markedly reduced in some areas. Calcified cartilage islands (arrow). (c) Irregularly dispersed hypertrophic cells hypertrophic chondrocytes with PAS-stained cytoplasmic inclusion bodies in chondrocytes. HE stain (b). PAS stain (c). Original magnification ×50 (b), ×200 (c).

the femora, and hypoplasia of iliac bones (Fig. 1a,b,c). The acetabular roofs were horizontal and arched with triangular ossification defects at the inferior aspect of the lateral iliac margin (Fig. 1c). After 3D-CT, a diagnosis of SRP type 3 was made prenatally based on Table 1. The parents chose cesarean section even after receiving full information regarding SRP type 3, and a male infant weighing 2328 g was delivered (Fig. 2a). The infant died of respiratory failure 3 h after birth. The skeletal manifestations on postmortem radiographs corresponded to those seen on 3D-CT (Fig. 1d,e; Table 1).

Macroscopic pathological examination at autopsy showed lung hypoplasia (left lung, 7.6 g; right lung, 10.0 g; lung/body weight ratio, 0.75%), hypoplasia of the bilateral kidneys, bilateral dilated ureter, hydropic scrotum, and absent penis (Fig. 2a). Chromosomal analysis using cultured lymphoblasts from cord blood showed a normal 46,XY karyotype.

Histological examination of growth plate cartilage at the costochondral junction revealed reduced numbers of resting and hypertrophic chondrocytes, a disorganized hypertrophic zone with loss of columnization, residual cartilaginous nests in the metaphyseal trabeculae, and PAS-positive intracytoplasmic inclusion bodies. Dispersed hypertrophic chondrocytes were separated by the normal cartilaginous matrix, but not by the fibrous tissue. Notably, calcified cartilage islands were observed in the metaphyseal trabeculae, and some were continuous with the physis through a narrow bridge (Fig. 2b,c). All of these histological findings were consistent with those of SRP type 3.[3–5]

Discussion

Measurement of fetal size, including femoral length, is currently a routine practice in obstetrics, facilitating identification of skeletal dysplasias with short limbs. Once limb shortening is identified, the subsequent diagnostic task involves assessment of the thorax to ascertain the presence or absence of thoracic hypoplasia, which allow determination of the clinical outcome of the fetus. Disorders that belong to the short-rib dysplasia group constitute a considerable portion of cases of skeletal dysplasia with thoracic hypoplasia. Prenatal diagnosis of short-rib dysplasia group using ultrasonography is feasible.[6–9] In the present case, the ultrasonography findings, including visceral anomalies, favored a diagnosis of SRP. However, detection of subtle skeletal abnormalities is generally difficult with

ultrasonography. Additional information on subsequent 3D-CT and MPR, including mild spondylar dysplasia, subtle metaphyseal changes, and irregular ossification defects in the outer iliac margin, eventually led to a diagnosis of SRP type 3 in this case.

Differential diagnosis between SRP, ATD, and EvC is difficult.[10,11] Antenatal diagnosis of SRP subtypes also appears difficult as there have been reports of common abnormalities, such as macrocephaly and polydactyly, as shown in Table 1. However, meticulous formulation of imaging findings on ultrasonography and 3D-CT helped in the prenatal diagnosis of SRP type 3 in the present case (Table 1). 3D-CT is particularly useful to delineate the axial skeleton. Although 3D image reconstruction tends to conceal fine bone details, such as mild metaphyseal dysplasia, this drawback was compensated by MPR (Fig. 1b). We evaluated the general skeletal structures first by 3D image reconstruction, and then examined the fine bone details by MPR, in which we were able to view any 2D images of bones as MPR and 3D images without rescanning independent of the fetal presentation.

The histological observations in the present case supported the suggestion that ATD type 1 and SRP type 3 may belong to the spectrum of the same pathogenetic entity.[3–5] In fact, mutations of *DYNC2H1* have recently been reported as a common cause of ATD and SRP3.[12] However, mutations of *IFT80* have also been reported as a cause of ATD, indicating genetic heterogeneity.[13]

In summary, the present case further exemplified the diagnostic capability of precise prenatal diagnosis of skeletal dysplasia. As shown in Table 1, meticulous interpretation of ultrasonography and CT imaging findings enabled us to subclassify SRP. To our knowledge, this is the first report of prenatal diagnosis in this group using 3D-CT.

References

1. Superti-Furga A, Unger S, The Nosology Group of the International Skeletal Dysplasia Society. Nosology and classification of genetic skeletal disorders: 2006 revision. *Am J Med Genet A* 2007; **143**: 1–18.
2. Cassart M, Massez A, Cos T *et al.* Contribution of three-dimensional computed tomography in the assessment of fetal skeletal dysplasia. *Ultrasound Obstet Gynecol* 2007; **29**: 537–543.
3. Yang SS, Langer LO Jr, Cacciarelli A *et al.* Three conditions in neonatal asphyxiating thoracic dysplasia (Jeune) and short rib-polydactyly syndrome spectrum: a clinicopathologic study. *Am J Med Genet Suppl* 1987; **3**: 191–207.
4. Erzen M, Stanescu R, Stanescu V *et al.* Comparative histopathology of the growth cartilage in short-rib polydactyly syndromes type I and type III and in chondroectodermal dysplasia. *Ann Genet* 1988; **31**: 144–150.
5. Hentze S, Sergi C, Troeger J *et al.* Short-rib-polydactyly syndrome type Verma-Naumoff-Le Marec in a fetus with histological hallmarks of type Saldino-Noonan but lacking internal organ abnormalities. *Am J Med Genet* 1998; **80**: 281–285.
6. Meizner I, Barnhard Y. Short-rib polydactyly syndrome (SRPS) type III diagnosed during routine prenatal ultrasonographic screening. A case report. *Prenat Diagn* 1995; **15**: 665–668.
7. Hill LM, Leary J. Transvaginal sonographic diagnosis of short-rib polydactyly dysplasia at 13 weeks' gestation. *Prenat Diagn* 1998; **18**: 1198–1201.
8. den Hollander NS, Robben SG, Hoogeboom AJ *et al.* Early prenatal sonographic diagnosis and follow-up of Jeune syndrome. *Ultrasound Obstet Gynecol* 2001; **18**: 378–383.
9. Viora E, Sciarrone A, Bastonero S *et al.* Three-dimensional ultrasound evaluation of short-rib polydactyly syndrome type II in the second trimester: a case report. *Ultrasound Obstet Gynecol* 2002; **19**: 88–91.
10. Golombeck K, Jacobs VR, von Kaisenberg C *et al.* Short rib-polydactyly syndrome type III: comparison of ultrasound, radiology, and pathology findings. *Fetal Diagn Ther* 2001; **16**: 133–138.
11. Spranger JW, Brill PW, Poznanski A (eds). *Bone Dysplasias*, 2nd edn. München: Oxford University Press: 2002; 15–21, 125–138.
12. Dagoneau N, Goulet M, Geneviève D *et al.* DYNC2H1 mutations cause asphyxiating thoracic dystrophy and short rib-polydactyly syndrome, type III. *Am J Hum Genet* 2009; **84**: 706–711.
13. Beales PL, Bland E, Tobin JL *et al.* IFT80, which encodes a conserved intraflagellar transport protein, is mutated in Jeune asphyxiating thoracic dystrophy. *Nat Genet* 2007; **39**: 727–729.

Journal of Human Genetics (2011) 56, 566–571

www.nature.com/jhg

ORIGINAL ARTICLE

Maternal age effect on the development of Prader–Willi syndrome resulting from upd(15)mat through meiosis 1 errors

Keiko Matsubara[1,2,3], Nobuyuki Murakami[2,3], Toshiro Nagai[2] and Tsutomu Ogata[1]

Prader–Willi syndrome (PWS) is primarily caused by deletions involving the paternally derived imprinted region at chromosome 15q11.2–q13 and maternal uniparental disomy 15 (upd(15)mat). The underlying mechanisms for upd(15)mat include trisomy rescue (TR), gamete complementation (GC), monosomy rescue and post-fertilization mitotic error, and TR/GC is mediated by non-disjunction at maternal meiosis 1 (M1) or meiosis 2 (M2). Of these factors involved in the development of upd(15)mat, M1 non-disjunction is a maternal age-dependent phenomenon. We studied 117 Japanese patients with PWS and identified deletions in 84 patients (Deletion group) and TR/GC type upd(15)mat through M1 non-disjunction in 15 patients (TR/GC (M1) group), together with other types of abnormalities. Maternal age was significantly higher in TR/GC (M1) group than in Deletion group (median (range), 37 (35–45) versus 30 (19–42); $P=1.0\times10^{-7}$). Furthermore, delayed childbearing age became obvious since the year 2003 in Japan, and relative frequency of TR/GC (M1) group was significantly larger in patients born since the year 2003 than in those born until the year 2002. The results imply that the advanced maternal age at childbirth is a predisposing factor for the development of upd(15)mat because of increased M1 errors.
Journal of Human Genetics (2011) **56**, 566–571; doi:10.1038/jhg.2011.59; published online 2 June 2011

Keywords: maternal age effect; meiosis 1; non-disjunction; Prader-Willi syndrome; upd(15)mat

INTRODUCTION

Prader–Willi syndrome (PWS) is a developmental disorder associated with various dysmorphic, neurologic, cognitive, endocrine and behavioral/psychiatric features.[1] It is caused by absent expression of paternally derived genes on the imprinted region at chromosome 15q11.2–q13, and previous studies have indicated that deletions of the paternally derived imprinted region and maternal uniparental disomy 15 (upd(15)mat) account for ~70 and ~25% of PWS patients, respectively.[1] The remaining PWS patients have rare abnormalities such as epimutations (hypermethylation) of the PWS imprinting center (IC), at the differentially methylated region encompassing exon 1 of *SNRPN* and microdeletions involving the PWS-IC or HBII-85 small nucleolar RNAs distal to the PWS-IC.[2–4]

Upd(15)mat are primarily caused by four mechanisms; that is, trisomy rescue (TR), gamete complementation (GC), monosomy rescue (MR) and post-fertilization mitotic error (PE).[5] TR refers to a condition in which chromosome 15 of paternal origin is lost from a zygote with trisomy 15, formed by fertilization between a disomic oocyte and a normal sperm. GC results from fertilization of a disomic oocyte with a nullisomic sperm. MR refers to a condition in which chromosome 15 of maternal origin is replicated in a zygote with monosomy 15, formed by fertilization between a normal oocyte and a nullisomic sperm. PE is an event after formation of a normal zygote. In this regard, a disomic oocyte specific to TR and GC is produced by non-disjunction at meiosis 1 (M1) or meiosis 2 (M2), and non-disjunction at M1 is known to increase with maternal age, probably because of a long-term (10–50 years) meiotic arrest at prophase 1.[6]

It is predicted, therefore, that the relative frequency of TR/GC-type upd(15)mat through M1 non-disjunction is high in PWS patients born to aged mothers and is increasing in countries where childbearing age is rising. In this context, previous studies have revealed a significantly higher maternal age in PWS patients with upd(15)mat than in those with deletions,[7,8] a significantly higher relative frequency of upd(15)mat in patients born to mothers aged ⩾35 years than in those born to mothers aged <35 years[9] and a significantly increased relative frequency of upd(15)mat in PWS patients <5 years of age in United Kingdom where childbearing age is increasing.[10] In these

[1]Department of Molecular Endocrinology, National Research Institute for Child Health and Development, Tokyo, Japan and [2]Department of Pediatrics, Dokkyo Medical University Koshigaya Hospital, Saitama, Japan
[3]These authors contributed equally to this work.
Correspondence: Dr T Ogata, Department of Molecular Endocrinology, National Research Institute for Child Health and Development, 2-10-1 Ohkura, Setagaya, Tokyo 157-8535, Japan.
E-mail: tomogata@nch.go.jp
Received 3 March 2011; revised 29 April 2011; accepted 8 May 2011; published online 2 June 2011

studies, however, as underlying mechanisms for upd(15)mat have not been examined, it remains to be clarified whether such maternal age effect on the occurrence of upd(15)mat is primarily mediated by M1 non-disjunction. Furthermore, after studying underlying mechanisms for upd(15)mat by microsatellite analysis, Robinson *et al.*[11] have mentioned that maternal age effect is similar between M1 and M2 errors. Thus, it remains to be clarified whether advanced maternal age is relevant to the occurrence of TR/GC type upd(15)mat through M1 errors.

Here, we report that the advanced maternal age at childbirth constitutes a risk factor for TR/GC type upd(15)mat through M1 non-disjunction.

MATERIALS AND METHODS

This study was approved by the Institute Review Board Committees at the National Center for Child Health and Development and Dokkyo University Koshigaya Hospital, and performed after obtaining informed consent.

PWS patients

This study consisted of 117 Japanese PWS patients (72 male patients and 45 female patients) who satisfied the following selection criteria: (1) normal karyotype in all the 50 lymphocytes examined, (2) hypermethylated PWS-IC that was confirmed by methylation analysis for bisulfite-treated leukocyte genomic DNA, using methylated and unmethylated allele-specific PCR primers (Supplementary Figure 1),[12] and (3) positive data on the maternal age at childbirth (parental age was not found in two aged patients who had left our follow-up and whose hospital records had been discarded and in one patient who was born after artificial insemination by donor).

Molecular studies

We performed fluorescence *in situ* hybridization analysis, microsatellite analysis and multiplex ligation-dependent probe amplification (MLPA) analysis. For fluorescence *in situ* hybridization analysis, an ~125-kb probe identifying a region encompassing *SNRPN* was hybridized to lymphocyte metaphase spreads, together with a CEP 15 probe for *D15Z1* and a probe for *PML* on 15q22 utilized as internal controls. The probe for the *SNRPN* region was labeled with digoxigenin and detected by rhodamine anti-digoxigenin, and the control probes were detected according to the manufacturer's protocol (Abbott, Chicago, IL, USA). For microsatellite genotyping, PCR amplification was performed for 13 microsatellite loci on chromosome 15, using fluorescently labeled forward primers and unlabeled reverse primers. Subsequently, the PCR products were determined for size on a CEQ8000 autosequencer (Beckman Coulter, Fullerton, CA, USA). For MLPA analysis, we utilized a commercially available MLPA probe mix (ME028-B1) for multiple segments on the chromosome 15 imprinted region, including the PWS-IC and three portions within the HBII-85 small nucleolar RNAs (MRC-Holland, Amsterdam, The Netherlands). The procedure was as described in the manufacturer's instructions. The primers utilized in this study are summarized in Supplementary Table 1.

Classification of PWS patients

The PWS patients were classified into several groups, according to the underlying (epi) genetic causes (Figure 1). In particular, upd(15)mat was divided into three groups by the previously reported methods[13] (Supplementary Figure 2): (1) heterodisomy for at least one of the three adjacent pericentromeric (<4 Mb from the centromere) microsatellite loci (*D15S541*, *D15S542* and *D15S1035*) was regarded as indicative of TR/GC type upd(15)mat through M1 non-disjunction (TR/GC (M1) group), (2) the combination of isodisomy for the pericentromeric microsatellite loci and heterodisomy for at least one middle to distal microsatellite loci was interpreted as indicative of TR/GC type upd(15)mat through M2 non-disjunction (TR/GC (M2) group) and (3) isodisomy for all the informative microsatellite loci was regarded as indicative of MR/PE type upd(15)mat (MR/PE group). However, it is usually impossible to distinguish between TR and GC, and between MR and PE on the basis of microsatellite data, although identification of segmental isodisomy or mosaicism with a normal cell lineage is unique to PE.[14,15]

Analysis of parental ages

We compared parental ages between different groups and between two different time periods (until the year 2002 and since the year 2003), and relative frequency of each group between the two time periods. The setting of the two time periods was based on the Annual Vital Statistics Data from the Japanese Ministry of Health, Labor and Welfare (http://www.mhlw.go.jp/toukei/list/81-1.html). The maternal age producing the largest number of live births changed from 25–29 years to 30–34 years, and that producing the third largest number of live births changed from 20–24 years to 35–39 years, between the two time periods (Supplementary Figure 3).

Statistical significance of the median age was examined by the Mann–Whitneys *U*-test, that of the correlation between parental ages by Spearman's rank correlation test, and that of relative frequency by the Fisher's exact probability test. $P<0.05$ was considered significant.

RESULTS

Classification of PWS patients

The results are shown in Figure 1. Fluorescence *in situ* hybridization analysis revealed heterozygous deletions in 84 of the 117 patients (Supplementary Figure 4;Deletion group). Then, microsatellite genotyping was carried out in 27 of the 33 patients without deletions, classifying 15 patients as TR/GC (M1) group, seven patients as TR/GC (M2) group and three patients as MR/PE group (Figure 2;in the remaining six patients, further studies were refused by the parents). There was no finding indicative of segmental isodisomy or mosaicism. Finally, MLPA was performed in the remaining two non-upd(15)mat patients, identifying no microdeletion affecting the PWS-IC. Thus, the two patients were classified as Epimutation group.

Analysis of parental ages

Distribution of parental ages in each group is shown in Figure 3a, and parental age data are summarized in Table 1. Maternal ages were invariably ⩾35 in TR/GC (M1) group. Furthermore, comparison of maternal ages in Deletion, TR/GC (M1) and TR/GC (M2) groups with >5 patients revealed significant difference between Deletion and TR/GC (M1) groups ($P=1.0\times10^{-7}$), but not between Deletion and TR/GC (M2) groups ($P=0.19$), and between TR/GC (M1) and TR/GC (M2) groups ($P=0.085$). Paternal ages showed similar tendency, with

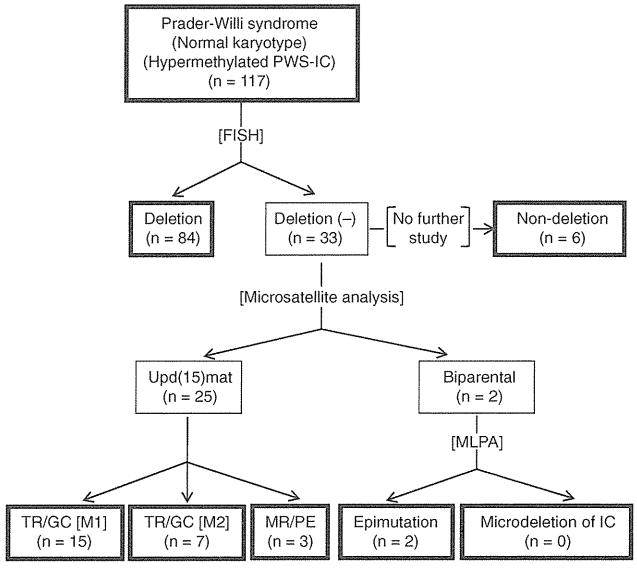

Figure 1 Classification of 117 Japanese patients with Prader–Willi syndrome phenotype.

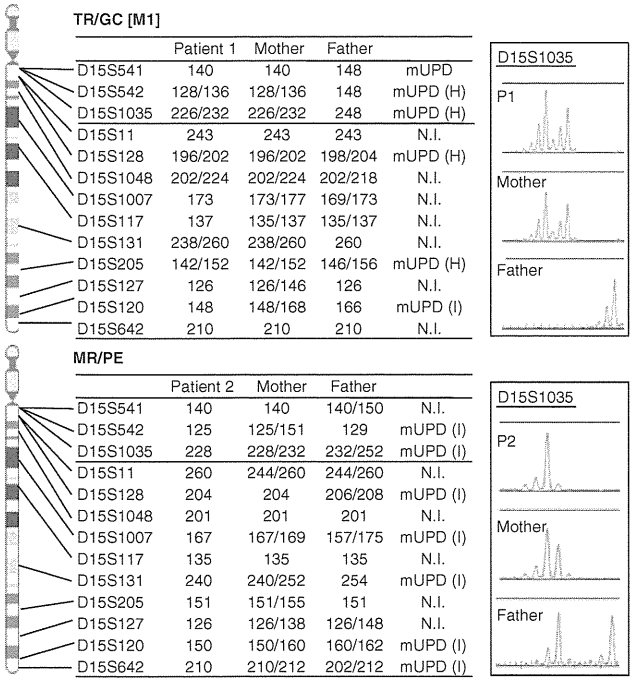

Figure 2 Chromosomal locations of the examined microsatellite loci and representative results. MUPD, maternal uniparental disomy (unknown for heterodisomy or isodisomy); mUPD (H), maternal uniparental heterodisomy; mUPD (I), maternal uniparental isodisomy; N.I., not informative. Pericentromeric loci are present in a heterodisomic status in patient 1, and this is consistent with trisomy rescue/gamete complementation (meiosis 1) (TR/GC (M1)) type maternal uniparental disomy 15 (upd(15)mat). For D15S1035, for example, both of the heterozygous maternal alleles are inherited by patient 1, whereas the homozygous paternal alleles are not transmitted to patient 1; this demonstrates mUPD (H) for this locus. In patient 2, all informative loci are present in an isodisomic condition, and this is compatible with monosomy rescue/post-fertilization mitotic error (MR/PE) type upd(15)mat. For D15S1035, for example, one of the two heterozygous maternal alleles is transmitted to patient 2, whereas both of the heterozygous paternal alleles are not inherited by patient 2; this demonstrates mUPD (I) for this locus.

significant difference between Deletion and TR/GC (M1) groups ($P=8.8\times10^{-5}$), but not between Deletion and TR/GC (M2) groups ($P=0.39$), and between TR/GC (M1) and TR/GC (M2) groups ($P=0.39$). However, whereas a significant correlation was observed between maternal and paternal ages in Deletion and TR/GC (M2) groups, there was no significant correlation between maternal and paternal ages in TR/GC (M1) group because of relatively advanced maternal ages in this group (Figure 3b). In addition, whereas maternal ages at childbirth were grossly similar between Deletion and TR/GC (M2) groups and the Japanese general population (the mean parental ages at childbirth in Japan were based on the data registered in the Ministry of Health, Labor and Welfare; http://www.mhlw.go.jp/toukei/list/81-1.html), they were obviously higher in TR/GC (M1) group than in the Japanese general population. Paternal ages at childbirth were grossly similar between Deletion group and the Japanese general population and tended to be higher in TR/GC (M1) and TR/GC (M2) groups than in the Japanese general population.

Relative frequency of each group markedly differed between 75 patients born until 2002 and 42 patients born since 2003 (Figure 3c). Here, TR/GC (M1) was indicated in three of the 75 patients born until the year 2002, and six non-deletion type patients were invariably born until the year 2002. Thus, TR/GC (M1) group accounted for at least three and up to nine of the 75 patients born until the year 2002, and 12 of the 42 patients born since the year 2003. Thus, the relative frequency of TR/GC (M1) was assessed to be significantly different, with the *P*-values being 1.8×10^{-7} for 3/75 versus 12/42, and 0.025 for 9/75 versus 12/42. In addition, there was no significant change in the parental ages of each group between the two time periods, although the maternal ages at birth of all the patients significantly differed between the two time periods.

DISCUSSION

The present study revealed deletions in 84 patients, upd(15)mat in 25 patients and epimutations in 2 patients. In addition, whereas microsatellite and MLPA analyses were not performed in six patients with non-deletion, the present and the previous studies argue that most of them have upd(15)mat, especially TR/GC (M1) type upd(15)mat.[1,13] Thus, the relative frequency of deletions, upd(15)mat and other rare causes appears to be similar between Japanese patient and previously reported Caucasian patients.[1]

Notably, the present study implies that advanced maternal age at childbirth constitutes a risk factor for the development of TR/GC (M1) type upd(15)mat. Indeed, maternal ages were significantly higher in TR/GC (M1) group than in Deletion group, which is free from maternal age effect. Although a significant difference was not found between maternal age-dependent TR/GC (M1) group and maternal age-independent TR/GC (M2) group, this would primarily be due to the small number of TR/GC (M2) group. Furthermore, the relative frequency of TR/GC (M1) group significantly increased since the year 2003 when delayed childbearing age became obvious, and the advanced maternal ages at birth since the year 2003 were primarily associated with the high frequency of TR/GC (M1) group rather than the advanced maternal ages in each group. Although it was impossible to distinguish between TR and GC, and between MR and PE,[16] this would not pose a major problem. The patients with M1 non-disjunction are included only in TR/GC (M1) group.

Paternal and environmental factors should also be considered for the present results. For a paternal factor, the frequencies of microdeletions and nullisomic sperms might increase with age.[17] However, paternal ages at childbirth in each group were similar between the two time periods, and the relative frequency of Deletion group actually decreased since the year 2003. Furthermore, whereas nullisomic sperms can be a background of the development of GC, concomitant occurrence of a nullisomic sperm and a disomic oocyte must be extremely rare. Rather, nullisomic sperms would primarily constitute an underlying factor for the development of maternal age-independent MR. For an environmental factor, it is predicted that chemical materials are increasing with time and that aged parents are exposed to such materials for a long time. In this regard, it has been reported that exposure to environmental chemicals may exaggerate the occurrence of aneuploidies in females.[18] Thus, the environmental factor might be relevant to the recent increase of TR/GC (M1) group, although it is unlikely that this factor constitutes the major cause of the increased TR/GC (M1) type upd(15)mat. In males, whereas it has been reported that exposure to chemical materials might facilitate the occurrence of PWS, the relative frequency of genetic causes remained unchanged in PWS patients born to such males.[19–21] Collectively, the effects of such non-maternal age factors would remain small, if any, although further careful examinations are required for the precise evaluation of the maternal age effect on the occurrence of TR/GC (M1).

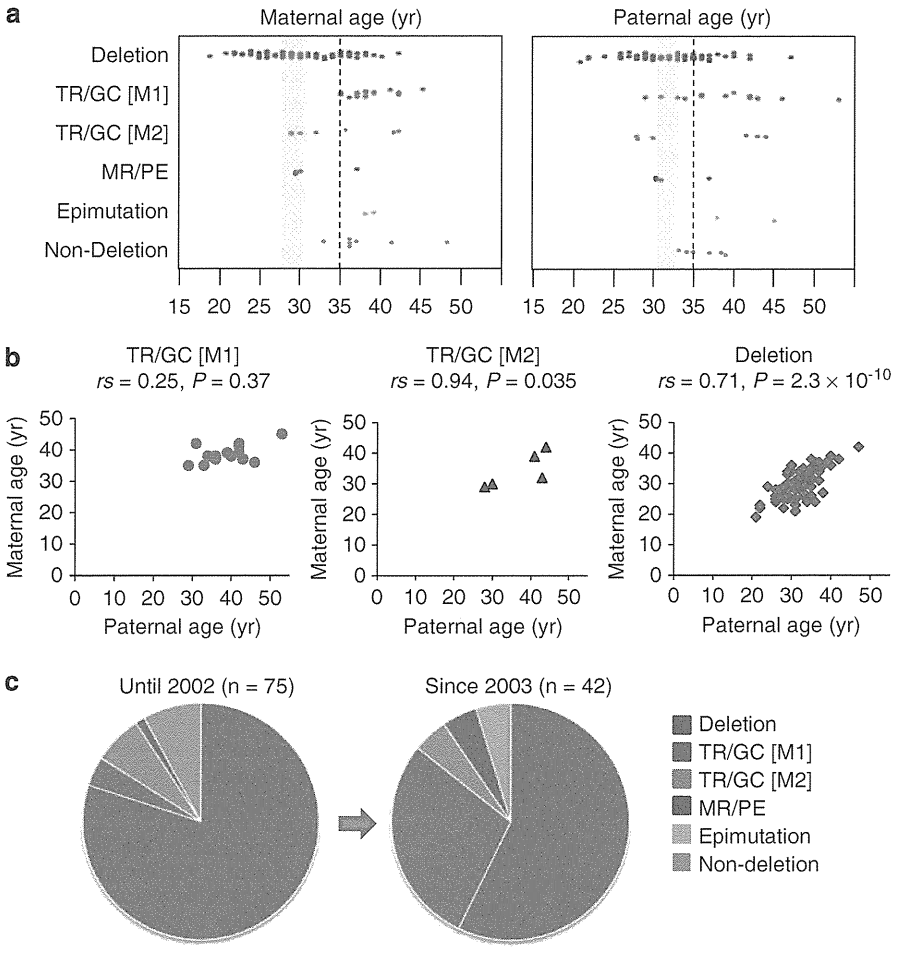

Figure 3 Analysis of parental ages at childbirth. (**a**) The distribution of parental ages in each group. The light pink and blue vertical bars represent the mean maternal and paternal ages at childbirth from the year 1970 to the year 2008. (**b**) Correlation between maternal and paternal ages at childbirth. Significant correlation is observed in trisomy rescue/gamete complementation (meiosis 2) (TR/GC (M2)) and Deletion groups, but not in trisomy rescue/gamete complementation (meiosis 1) (TR/GC (M1)) group because of relatively advanced maternal age. (**c**) Relative frequency of each group in 75 patients born until the year 2002 (n=60, 3, 5, 1, 0 and 6 for Deletion, TR/GC (M1), TR/GC (M2), monosomy rescue/post-fertilization mitotic error (MR/PE), epimutation and non-deletions groups, respectively) and in 42 patients born since the year 2003 (n=24, 12, 2, 2, 2 and 0 for Deletion, TR/GC (M1), TR/GC (M2), MR/PE, Epimutation and Non-deletions groups, respectively).

Several points should be made with regard to the present study. First, we classified upd(15)mat primarily on the basis of the results of three pericentromeric microsatellite loci, with the assumption of no recombination between the centromere and the three loci, as have been employed in the previous study.[13] The methods would be basically acceptable, because the three loci reside within a 4 Mb region from the centromere and a recombination is relatively rare in the centromeric regions.[22] However, it remains possible that a cryptic recombination(s) might have occurred in the pericentromeric region.

Second, upd(15)mat may also be caused by maternal age-dependent meiotic sister chromatid pre-division that can lead to aneuploid oocytes, including disomic oocytes specific to TR/GC.[23] In this regard, as such disomic oocytes can have various patterns of isodisomic and heterodisomic regions, it is impossible to discriminate between upd(15)mat through sister chromatid pre-division and that through conventional meiotic non-disjunction by microsatellite analysis. Thus, the patients classified as TR/GC (M1) group may have upd(15)mat due to maternal age-dependent conventional non-disjunction at M1 and maternal age-dependent sister chromatid pre-division, whereas those classified as TR/GC (M2) group may have upd(15)mat due to maternal age-independent conventional non-disjunction at M2 and maternal age-dependent sister chromatid pre-division. However, even if not all the patients classified as TR/GC (M1) group have upd(15)mat due to conventional non-disjunction at M1, it can be concluded that maternal age-dependent factors still have a critical role in the occurrence of upd(15)mat in patients classified as TR/GC (M1) group. In addition, possible mixture of maternal age-dependent and -independent factors in patients classified as TR/GC (M2) group may be relevant to the lack of significant difference in the maternal age between TR/GC (M2) and Deletion groups, and between TR/GC (M2) and TR/GC (M1) groups.

Lastly, whereas fluorescence *in situ* hybridization analysis has been routinely performed at commercial laboratories since the year 1993 in Japan, detailed molecular studies including microsatellite analysis are usually available only in institutional laboratories. Thus, a substantial fraction of patients without deletions may have remained undiagnosed or misdiagnosed, without receiving further studies including micro-

Table 1 Parental ages (year) at childbirth

	Deletion	*TR/GC (M1)*	*TR/GC (M2)*	*MR/PE*	*Epimutation*	*Non-deletion*	*All patients*	*General population*
Maternal age								
Total								
Median	30	37	31	30	38.5	36	32	27.5–30.9
Range	19–42	35–45	29–42	29–37	38–39	30–48	19–48	
Number	84	15	7	3	2	6	117	
Until 2002								
Median	29	37	32	29	—	36	30[a]	
Range	19–42	35–37	29–42	—	—	30–48	19–48	
Number	60	3	5	1	0	6	75	
Since 2003								
Median	32.5	38.5	35.5	33.5	38.5	—	35[a]	
Range	23–39	35–45	30–41	30–37	38–39	—	23–45	
Number	24	15	2	2	2	0	42	
Paternal age								
Total								
Median	32.5	40	35.5	31	41.5	36	33	30.6–33.0
Range	21–47	29–53	28–44	28–37	38–45	33–39	21–53	
Number	82[b]	15	6[c]	3	2	6	114[b,c]	
Until 2002								
Median	32.5	43	35.5	28	—	36	33	
Range	21–47	33–43	28–44	—	—	33–39	21–47	
Number	58[b]	3	4[c]	1	0	6	72[b,c]	
Since 2003								
Median	32.5	39.5	35.5	34	41.5	—	34.5	
Range	22–40	29–53	30–41	31–37	38–45	—	22–53	
Number	24	12	2	2	2	0	42	

Abbreviations: GC, gamete complementation; M1, meiosis 1; M2, meiosis 2; MR,monosomy rescue; PE, post-fertilization mitotic error; TR, trisomy rescue.
The data of the general population indicate the range of the mean parental ages at childbirth from the year 1970 to 2008.
[a]*P*-value=0.00017.
[b]Paternal age was not found in two old patients who had left our follow-up and whose hospital records had been discarded.
[c]Paternal age was not identified in one patient who was born after artificial insemination by donor.

satellite analysis at appropriate institutions. In this regard, considering the opportunity to receive detailed molecular studies, it is possible that upd(15)mat is overlooked more frequently in aged patients than in young patients. If so, this may be relevant to the significant difference in the relative frequency of TR/GC (M1) group between the two time periods ('since the year 2003' versus 'until the year 2002').

In summary, the results imply that the advanced maternal age at childbirth is a predisposing factor for the development of upd(15)mat because of increased M1 errors. This notion is applicable to maternal upd in general, as well as to trisomies. However, there are several caveats as discussed in the above, and the number of patients, especially those classified as TR/GC (M2) group, is small. Thus, further careful studies using a large number of patients are necessary in the future.

CONFLICT OF INTEREST

The authors declare no conflict of interest.

ACKNOWLEDGEMENTS

This work was supported by Grants for Research on Intractable Diseases (H22-165) and for Health Research on Children, Youth and Families (H21-005) from the Ministry of Health, Labor and Welfare, and by Grants-in-Aid for Scientific Research (A) (22249010) and Grant-in-Aid for Young Scientists (B) (22791022) from the Japan Society for the Promotion of Science (JSPS).

1 Cassidy, S. B. & Driscoll, D. J. Prader-Willi syndrome. *Eur. J. Hum. Genet.* **17,** 3–13 (2009).
2 Buiting, K., Grob, S., Lich, C., Gillessen-Kaesbach, G., El-Maarri, O. & Horsthemke, B. Epimutation in Prader-Willi and Angelman syndromes: a molecular study of 136 patients with an imprinting defect. *Am. J. Hum. Genet.* **72,** 571–577 (2003).
3 Sahoo, T., del Gaudio, D., German, J. R., Shinawi, M., Peter, S. U., Person, R. E. *et al.* Prader-Willi phenotype caused by paternal deficiency for the HBII-85 C/D box small nucleolar RNA cluster. *Nat. Genet.* **40,** 719–721 (2008).
4 de Smith, A. J., Purmann, C., Walters, R. G., Ellis, R. J., Holder, S. E., VanHaelst, M. *et al.* A deletion of the HBII-85 class of small nucleolar RNAs (snoRNAs) is associated with hyperphagia, obesity and hypogonadism. *Hum. Mol. Genet.* **18,** 3257–3265 (2009).
5 Shaffer, L. G., Agan, N., Goldberg, J. D., Ledbetter, D. H., Longshore, J. W. & Cassidy, S. B. American College of Medical Genetics statement on diagnostic testing for uniparental disomy. *Genet. Med.* **3,** 206–211 (2001).
6 Jones, K. T. Meiosis in oocytes: predisposition to aneuploidy and its increased incidence with age. *Hum. Reprod. Update.* **14,** 143–158 (2008).
7 Mitchell, J., Schinzel, A., Langlois, S., Gillessen-Kaesbach, G., Schuffenhauer, S., Michaelis, R. *et al.* Comparison of phenotype in uniparental disomy and deletion Prader-Willi syndrome: sex specific differences. *Am. J. Med. Genet.* **65,** 133–136 (1996).
8 Cassidy, S. B., Forsythe, M., Heeger, S., Nicholls, R. D., Schork, N., Benn, P. *et al.* Comparison of phenotype between patients with Prader-Willi syndrome due to deletion 15q and uniparental disomy 15. *Am. J. Med. Genet.* **68,** 433–440 (1997).
9 Ginsburg, C., Fokstuen, S. & Schinzel, A. The contribution of uniparental disomy to congenital development defects in children born to mothers at advanced childbearing age. *Am. J. Med. Genet.* **95,** 454–460 (2000).
10 Whittington, J. E., Butler, J. V. & Holland, A. J. Changing rates of genetic subtypes of Prader-Willi syndrome in the UK. *Eur. J. Hum. Genet.* **15,** 127–130 (2007).
11 Robinson, W. P., Langlois, S., Schuffenhauer, S., Horsthemke, B., Michaelis, R. C., Christian, S. *et al.* Cytogenetic and age-dependent risk factors associated with uniparental disomy 15. *Prenat. Diagn.* **16,** 837–844 (1996).

12 Kubota, T., Das, S., Cristian, S. L., Baylin, S. B., Herman, J. G. & Ledbetter, D. H. Methylation-specific PCR simplifies imprinting analysis. *Nat. Genet.* **16,** 16–17 (1997).
13 Robinson, W. P., Kuchinka, B. D., Bernasconi, F., Peterson, M. B., Schulze, A., Brondum-Nielsen, K. *et al.* Maternal meiosis I non-disjunction of chromosome 15: dependence of the maternal age effect on level of recombination. *Hum. Mol. Genet.* **7,** 1011–1019 (1998).
14 Robinson, W. P. Mechanisms leading to uniparental disomy and their clinical consequences. *Bioessays* **22,** 452–459 (2000).
15 Kotzot, D. Advanced parental age in maternal uniparental disomy (UPD): implications for the mechanism of formation. *Eur. J. Hum. Genet.* **12,** 343–346 (2004).
16 Oliver, T. R., Feingold, E., Yu, K., Cheung, V., Tinker, S., Yadav-Shah, M. *et al.* New insights into human nondisjunction of chromosome 21 in oocytes. *PLoS Genet.* **4,** e1000033 (2008).
17 Sloter, E., Nath, J., Eskenazi, B. & Wyrobek, A. J. Effects of male age on the frequencies of germinal and heritable chromosomal abnormalities in humans and rodents. *Fertil. Steril.* **81,** 925–943 (2004).
18 Pacchierotti, F., Adler, I. D., Eichenlaub-Ritter, U. & Mailhes, J. B. Gender effects on the incidence of aneuploidy in mammalian germ cells. *Environ. Res.* **104,** 46–69 (2007).
19 Strakowski, S. M. & Butler, M. G. Paternal hydrocarbon exposure in Prader-Willi syndrome. *Lancet* **330,** 1458 (1987).
20 Cassidy, S. B., Gainey, A. J. & Butler, M. G. Occupational hydrocarbon exposure among fathers of Prader-Willi syndrome patients with and without deletions of 15q. *Am. J. Hum. Genet.* **44,** 806–810 (1989).
21 Akefeldt, A., Anvret, M., Grandell, U., Nordlinder, R. & Gillberg, C. Parental exposure to hydrocarbons in Prader-Willi syndrome. *Dev. Med. Chil. Neurol.* **37,** 1101–1109 (1995).
22 Robinson, W. P., Bernasconi, F., Mutirangura, A., Ledbetter, D. H., Langlois, S., Malcom, S. *et al.* Nondisjunction of chromosome 15: origin and recombination. *Am. J. Hum. Genet.* **53,** 740–751 (1993).
23 Pellestor, F., Andreo, B., Anahory, T. & Hamamah, S. The occurrence of aneuploidy in human: lessons from the cytogenetic studies of human oocytes. *Eur. J. Med. Genet.* **49,** 103–116 (2006).

Supplementary Information accompanies the paper on Journal of Human Genetics website (http://www.nature.com/jhg)

RESEARCH LETTER

AMERICAN JOURNAL OF medical genetics PART A

Mosaic upd(7)mat in a Patient With Silver–Russell Syndrome

Tomoko Fuke-Sato,[1,2] Kazuki Yamazawa,[1] Kazuhiko Nakabayashi,[3] Keiko Matsubara,[1] Kentaro Matsuoka,[4] Tomonobu Hasegawa,[2] Kazushige Dobashi,[5] and Tsutomu Ogata[1,6]*

[1]Department of Molecular Endocrinology, National Research Institute for Child Health and Development, Tokyo, Japan

[2]Department of Pediatrics, Keio University School of Medicine, Tokyo, Japan

[3]Department of Maternal-Fetal Biology, National Research Institute for Child Health and Development, Tokyo, Japan

[4]Division of Pathology, National Medical Center for Children and Mothers, Tokyo, Japan

[5]Department of Pediatrics, Showa University School of Medicine, Tokyo, Japan

[6]Department of Pediatrics, Hamamatsu University School of Medicine, Hamamatsu, Japan

Received 10 March 2011; Accepted 9 November 2011

TO THE EDITOR:

Silver–Russell syndrome (SRS) is a congenital developmental disorder characterized by pre- and post-natal growth failure, relative macrocephaly, triangular face, hemihypotrophy, and 5th finger clinodactyly[Q2] [Russell, 1954; Silver et al., 1953]. Recent studies have shown that hypomethylation (epimutation) of the paternally derived differentially methylated region (DMR) in the upstream of *H19* (*H19*-DMR) on chromosome 11p15 and maternal uniparental disomy for chromosome 7 (upd(7)mat) account for ~45% and ~5–10% of SRS patients, respectively [Eggermann, 2010; Binder et al., 2011]. Furthermore, consistent with the involvement of imprinted genes in both body and placental growth [for review, Coan et al., 2005], epimutations of the *H19*-DMR and upd(7)mat are known to result in placental hypoplasia [Yamazawa et al., 2008a,b]. Here, we report on a Japanese boy with mosaic upd(7)mat)mat who was identified through genetic screenings in 120 patients with SRS-like phenotype.

This Japanese boy was conceived naturally to a 41-year-old father and a 36-year-old mother. The parents were non-consanguineous and healthy. The paternal height was 165 cm (−0.9 SD), and the maternal height 155 cm (−0.6 SD).

At 35 weeks of gestation, he was delivered by a cesarean because of fetal distress. At birth, his length was 37.4 cm (−3.1 SD), his weight 1.28 kg (−3.1 SD), and his head circumference 29.0 cm (−1.3 SD). The placenta weighed 400 g (−0.6 SD [Kagami et al., 2008]). Shortly after birth, he was found to have ventricular septal defect, hydronephrosis, and abnormal external genitalia (hypospadias, bifid scrotum, and bilateral cryptorchidism). He received orchidopexy at $1^{10}/_{12}$ years of age and genitoplasty at $2^{4}/_{12}$ years of age. He exhibited feeding difficulty and speech delay.

At $5^{1}/_{12}$ years of age, he was referred because of short stature. His height was 87.9 cm (−4.3 SD), weight was 10.4 kg (−2.9 SD), and his head circumference 49.0 cm (−0.7 SD). Physical examination showed relative macrocephaly, abnormal teeth, 5th finger clinodactyly, and underdeveloped muscles. There was no hemihypotrophy. Endocrine studies for short stature yielded normal results, as did radiological examinations. His karyotype was 46,XY in all the 50 lymphocytes examined. He was clinically diagnosed as having SRS, and molecular studies were performed after obtaining the approval from the Institutional Review Board Committee at National Center for Child Health and Development and the written informed consent from the parents.

We first performed methylation analysis of the *MEST*-DMR on chromosome 7q32.2 using leukocyte genomic DNA by the previously described methods [Yamazawa et al., 2008b], because this patient showed relatively mild SRS-phenotype with speech delay

How to Cite this Article:
Fuke-Sato T, Yamazawa K, Nakabayashi K, Matsubara K, Matsuoka K, Hasegawa T, Dobashi K, Ogata T. 2011. Mosaic upd(7)mat in a patient with Silver–Russell syndrome. Am J Med Genet Part A 9999:1–4.

Grant sponsor: Japan[Q1] Society for the Promotion of Science (JSPS); Grant number: 22249010; Grant sponsor: Ministry of Health, Labor and Welfare; Grant number: H21-005; Grant sponsor: Grant of National Center for Child Health and Development; Grant number: 23A-1.

*Correspondence to:
Tsutomu Ogata, M.D., Department of Pediatrics, Hamamatsu University School of Medicine, Hamamatsu 431-3192, Japan.
E-mail: tomogata@hama-med.ac.jp

Published online 00 Month 2011 in Wiley Online Library (wileyonlinelibrary.com).
DOI 10.1002/ajmg.a.34404

and feeding difficulty characteristic of upd(7)mat [Hitchins et al., 2001; Kotzot, 2008]. The methylation analysis showed a major peak for methylated clones and a minor peak for unmethylated clones in this patient (Fig. 1A). We also examined the *H19*-DMR and other multiple DMRs on various chromosomes by the bio-COBRA (combined bisulfite restriction analysis) method, as reported previously [Yamazawa et al., 2010]. The *GRB10*-DMR on chromosome 7p12.1 and the *PEG10*-DMR on chromosome 7q21.3 exhibited skewed methylation patterns consistent with the predominance of maternally derived clones, as did the *MEST*-DMR (Fig. 1B). By

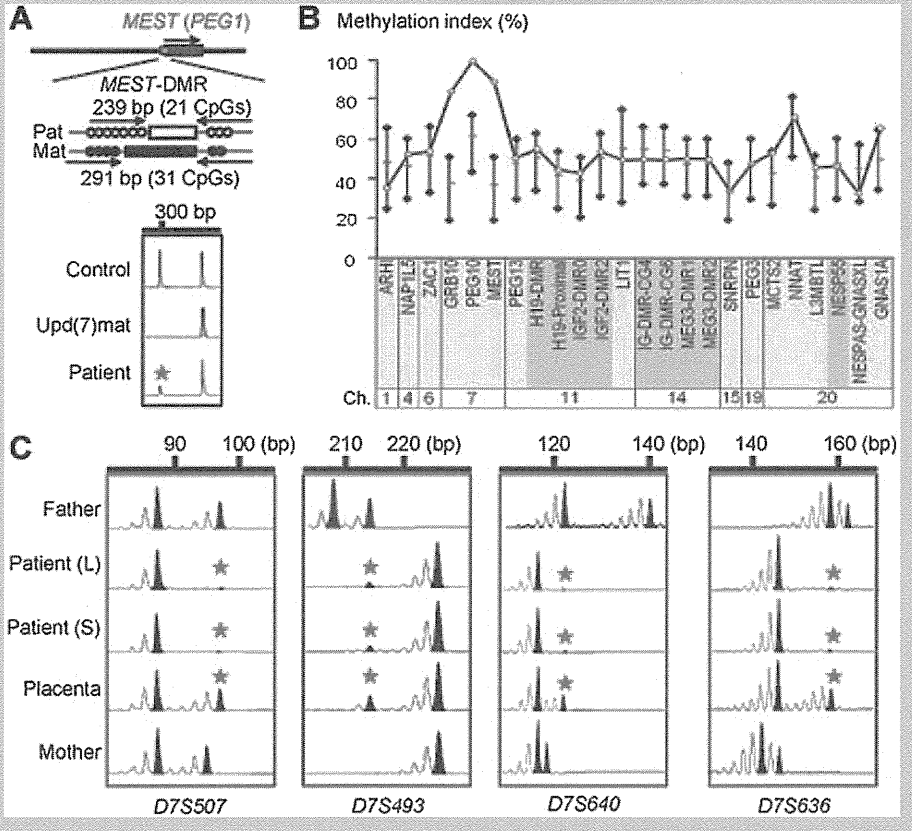

FIG. 1. Representative molecular results. A: Methylation analysis for the *MEST*-DMR. The methylated and unmethylated allele-specific primers were designed to yield PCR products of different sizes, and the PCR products were visualized on the 2100 Bioanalyzer (Agilent, Santa Clara, CA). Both methylated and unmethylated alleles are amplified in a control subject, and the methylated allele only is identified in a previously reported patient with upd(7)mat [Yamazawa et al., 2008b]. In this patient, a major peak for the methylated allele and a minor peak for the unmethylated allele (a red asterisk) are delineated. B: Methylation indices of 24 DMRs examined by the bio-COBRA. The PCR products were digested with methylation sensitive restriction enzymes, and the methylation indices (the ratios of methylated clones) were calculated using peak heights of digested and undigested fragments on the 2100 Bioanalyzer using 2100 expert software. The black vertical bars indicate the reference data in 20 normal control subjects (maximum – minimum). The DMRs highlighted in blue and pink are methylated after paternal and maternal transmissions, respectively.
C: Microsatellite analysis. Major peaks of maternal origin and minor peaks of paternal origin (red asterisks) are identified in this patient. The minor peaks of paternal origin are more obvious in the placenta than in the leukocytes (L) and salivary cells (S). Calculation of the mosaic ratio using the *D7S507* data, under the assumption of no trisomic cells. For this locus, the patient is considered to be heterozygous with the major 87 bp peak of maternal origin and a minor 97 bp peak of paternal origin. The father is also heterozygous with the two peaks of the same sizes, and the area under curve (AUC) is larger for the short 87 bp peak than for the long 97 bp peak. This unequal amplification is consistent with short products being more easily amplified than long products. In this patient, the AUC ratio between the major 87 bp peak and the minor 97 bp peak is obtained as 1.0:0.043 for leukocytes, 1.0:0.044 for salivary cells, and 1.0:0.803 in placental tissue, after compensation of the unequal amplification between the two peaks using the paternal data. Here, let "XL" represent the frequency of the upid(7)mat cells in leukocytes (thus, (1 – XL) denotes the frequency of normal cells in leukocytes). Then, the paternally derived 97 bp peak is generated by one paternally derived chromosome in the normal cells, that is, (1 – XL), and the maternally derived 87 bp peak is formed by the products from two maternally derived homologous chromosomes in the upid(7)mat cells and one maternally derived chromosome in the normal cells, that is, {2XL + (1 – XL)} = (XL + 1). Thus, the AUC ratio between the two peaks is represented as (XL + 1):(1 – XL) = 1.0:0.043, and "XL" is calculated as 0.92 (92%). Similarly, when "XS" and "XP" represent the frequency of the upid(7)mat cells in salivary cells and placental tissue, respectively, "XS" is obtained as 0.91 (91%) and "XP" as 0.11 (11%). Furthermore, when "XB" represents the frequency of the upid(7)mat cells in buccal epithelium cells, "XB" is obtained as 0.91 (91%), on the basis of the previous report that salivary cells comprises ~40% of buccal epithelium cells and ~60% of leukocytes [Thiede et al., 2000].

TABLE I. The Results of Microsatellite Analysis

Locus	Position	Father	Patient (L)	Patient (S)	Placenta	Mother	Assessment
D7S517	7p22.2	254/258	(254)/258	(254)/258	(254)/258	256/258	Maternal Iso-D[a]/biparental
D7S507	7p15–21	87/97	87/(97)	87/(97)	87/(97)	87/95	Maternal Iso-D[a]/biparental
D7S493	7p15.3	208/214	(214)/226	(214)/226	(214)/226	226	Maternal D[b]/biparental
D7S484	7p14–15	96/100	(96)/98	(96)/98	(96)/98	98/100	Maternal Iso-D/biparental
D7S502	7q11.12	298	294/(298)	294/(298)	294/(298)	294/304	Maternal Iso-D/biparental
D7S669	7q11.2	116/126	(116)/124	(116)/124	(116)/124	124	Maternal D[b]/biparental
D7S515	7q21–22	169/173	171/(173)	171/(173)	171/(173)	169/171	Maternal Iso-D/biparental
D7S640	7q21.1–31.2	122/140	116/(122)	116/(122)	116/(122)	116/118	Maternal Iso-D/biparental
D7S684	7q34	169/179	177/(179)	177/(179)	177/(179)	177/179	Not informative
D7S636	7q35–36	158/162	146/(158)	146/(158)	146/(158)	142/146	Maternal Iso-D/biparental
D7S798	7q36	73/79	(79)/83	(79)/83	(79)/83	73/83	Maternal Iso-D/biparental

L, leukocytes; S, salivary cells; D, disomy.
The Arabic numbers denote the PCR product sizes in bp.
The minor peaks are indicated in parentheses.
[a]On the basis of the results of other informative loci, the major peaks are considered to be of maternal origin.
[b]Because of the maternal homozygosity, disomic status (isodisomy or heterodisomy) is unknown for these loci.

contrast, other DMRs including the *H19*-DMR showed normal methylation patterns.

We next performed microsatellite analysis for 11 loci on various parts of chromosome 7, using genomic DNA from leukocytes of the patient and the parents, from salivary cells of the patient, and from formalin-fixed and paraffin-embedded placental tissue. Major peaks consistent with maternal uniparental isodisomy and minor peaks of paternal origin were unequivocally identified for *D7S484*, *D7S502*, *D7S515*, *D7S640*, *D7S636*, and *D7S798*; furthermore, similar patterns were also detected for *D7S517*, *D7S507*, *D7S669*, and *D7S493*, although the results were not informative for *D7S684* (Fig. 1C and Table I). The minor peaks of paternal origin were similar between leukocytes and salivary cells and more evident in placental tissue. These findings, together with the normal karyotype in lymphocytes, indicated mosaic full maternal isodisomy for chromosome 7 (upid(7)mat) in this patient. Furthermore, since such a condition is frequently associated with mosaicism for trisomy 7 [Petit et al., 2011], we performed fluorescence in situ hybridization (FISH) analysis for stocked lymphocyte pellets, using a CEP7 probe for *D7Z1* (Abbott[Q3]). The FISH analysis identified two normal signals in 995 of 1,000 interphase nuclei examined, with no trace of trisomic nuclei; while a single signal was delineated in the remaining five nuclei, this was regarded as a false-positive finding. Thus, assuming no trisomic cells, the frequency of the full upid(7)mat cells was calculated as 92% in leukocytes, using the results of *D7S507* (Fig. 1C). In addition, similarly assuming no trisomic cells in other tissues, the frequency of the full upid(7)mat cells was calculated as 91% salivary cells (and in buccal cells) and 11% in placental tissue, although we could not perform FISH analysis in buccal cells and placental cells.

These results imply that this patient had an abnormal cell lineage with full upid(7)mat and a normal cell lineage with biparentally inherited chromosome 7 homologs at least in lymphocytes, and these had no trisomy 7. It is likely that mitotic non-disjunction and subsequent trisomy rescue (loss of the paternally derived chromosome 7 from a trisomic cell) took place in the post-zygotic developmental stage, resulting in the production of the mosaic full upid(7)mat (Fig. 2). While full upid(7)mat can also be produced by monosomy rescue (duplication of a single maternally derived chromosome 7 in a zygote), this mechanism is predicted to cause non-mosaic rather than mosaic upid(7)mat [Miozzo et al., 2001]. Although it remains to be clarified why trisomic cells mediating the production of full upid(7)mat cells were apparently absent in lymphocytes of this patient, there might be a negative selection against lymphocytes with trisomy 7.

However, the presence or absence of demonstrable trisomic cells was studied only in lymphocytes. In this regard, trisomic cells have been identified more frequently in skin fibroblasts and amniocytes than in blood cells in patients with mosaic trisomy 7 [Chen et al., 2010; Petit et al., 2011], and they are usually more frequently detected in the placental tissue than in the body tissue, as has been demonstrated by confined placental trisomy [Kalousek et al., 1991]. These findings would argue for the possible presence of trisomic cells in several tissues including placenta of this patient.

The full upid(7)mat cells were assessed to account for the majority of the leukocytes and salivary cells (buccal cells) and the minority of the placental tissue, under the assumption of no

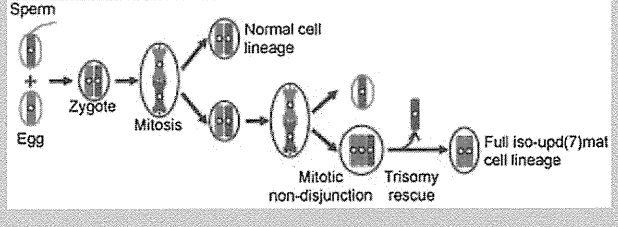

FIG. 2. Schematic representation of the generation of the mosaic upid(7)mat. The maternally and paternally derived chromosome 7 homologs are shown in red and blue, respectively. In this figure, mitotic non-disjunction is assumed at the second mitosis.

trisomic cells. In this regard, if trisomic cells may be present in a certain fraction of buccal cells and placental tissue, the full upid-(7)mat cells would still account for a relatively major fraction of buccal cells and a relatively minor fraction of the placental cells. While such a variation in the frequency of the full upid(7)mat cells among different tissues would primarily be a stochastic event, it should be pointed out that human genetic studies are usually performed for leukocytes. Indeed, if the upid(7)mat cells were barely present in leukocytes, the mosaic upid(7)mat would not have been detected. Such a bias in human studies would more or less be relevant to the relative predominance of the full upid(7)mat cells in leukocytes.

Two findings are noteworthy with regard to clinical features of this patient. First, this patient had relatively mild SRS phenotype with speech delay and feeding difficulty. Since such clinical features are grossly consistent with those of patients with upd(7)mat [Hitchins et al., 2001; Kotzot, 2008], it is inferred that the upid-(7)mat cells accounted for a considerable fraction of body cells relevant to the development of SRS phenotype. Second, the placental size remained within the normal range. This would be consistent with the relative paucity of the upid(7)mat cells in the placenta.

In summary, we observed mosaic upid(7)mat in a patient with SRS. Further studies will identify mosaic upd(7)mat with or without demonstrable trisomy 7 in patients with relatively mild SRS-like phenotype.

ACKNOWLEDGMENTS

This work was supported by the Grant-in-Aid for Scientific Research (A) (22249010) from the Japan Society for the Promotion of Science (JSPS), by the Grants for Health Research on Children, Youth, and Families (H21-005) from the Ministry of Health, Labor and Welfare, and by the Grant of National Center for Child Health and Development (23A-1).

REFERENCES

Binder G, Begemann M, Eggermann T, Kannenberg K. 2011. Silver-Russell syndrome. Best Pract Res Clin Endocrinol Metab 25:153–160.

Chen CP, Su YN, Chern SR, Hwu YM, Lin SP, Hsu CH, Tsai FJ, Wang TY, Wu PC, Lee CC, Chen YT, Chen LF, Wang W. 2010. Mosaic trisomy 7 at amniocentesis: Prenatal diagnosis and molecular genetic analyses. Taiwan J Obstet Gynecol 49:333–340.

Coan PM, Burton GJ, Ferguson-Smith AC. 2005. Imprinted genes in the placenta: A review. Placenta 26:S10–S20.

Eggermann T. 2010. Russell–Silver syndrome. Am J Med Genet Part C 154C:355–364.

Hitchins MP, Stanier P, Preece MA, Moore GE. 2001. Silver-Russell syndrome: A dissection of the genetic aetiology and candidate chromosomal regions. J Med Genet 38:810–819.

Kagami M, Yamazawa K, Matsubara K, Matsuo N, Ogata T. 2008. Placentomegaly in paternal uniparental disomy for human chromosome 14. Placenta 29:760–761.

Kalousek DK, Howard-Peebles PN, Olson SB, Barrett IJ, Dorfmann A, Black SH, Schulman JD, Wilson RD. 1991. Confirmation of CVS mosaicism in term placentae and high frequency of intrauterine growth retardation association with confined placental mosaicism. Prenat Diagn 11:743–750.

Kotzot D. 2008. Maternal uniparental disomy 7 and Silver–Russell syndrome—Clinical update and comparison with other subgroups. Eur J Med Genet 51:444–451.

Miozzo M, Grati FR, Bulfamante G, Rossella F, Cribiù M, Radaelli T, Cassani B, Persico T, Cetin I, Pardi G, Simoni G. 2011. Post-zygotic origin of complete maternal chromosome 7 isodisomy and consequent loss of placental *PEG1/MEST* expression. Placenta 22:813–821.

Petit F, Holder-Espinasse M, Duban-Bedu B, Bouquillon S, Boute-Benejean O, Bazin A, Rouland V, Manouvrier-Hanu S, Delobel B. 2011. Trisomy 7 mosaicism prenatally misdiagnosed and maternal uniparental disomy in a child with pigmentary mosaicism and Russell–Silver syndrome. Clin[Q4] Genet [Epub ahead of print], PHID: 21204802.

Russell A. 1954. A syndrome of intra-uterine dwarfism recognizable at birth with cranio-facial dysostosis, disproportionately short arms and other anomalies. Proc R Soc Med 47:1040–1044.

Silver HK, Kiyasu W, George J, Deamer WC. 1953. Syndrome of congenital hemihypertrophy, shortness of stature, and elevated urinary gonadotrophins. Pediatrics 12:368–375.

Thiede C, Prange-Krex G, Freiberg-Richter J, Bornhäuser M, Ehninger G. 2000. Buccal swabs but not mouthwash samples can be used to obtain pretransplant DNA fingerprints from recipients of allogeneic bone marrow transplants. Bone Marrow Transplant 25:575–577.

Yamazawa K, Kagami M, Nagai T, Kondoh T, Onigata K, Maeyama K, Hasegawa T, Hasegawa Y, Yamazaki T, Mizuno S, Miyoshi Y, Miyagawa S, Horikawa R, Matsuoka K, Ogata T. 2008a. Molecular and clinical findings and their correlations in Silver-Russell syndrome: Implications for a positive role of IGF2 in growth determination and differential imprinting regulation of the *IGF2-H19* domain in bodies and placentas. J Mol Med 86:1171–1181.

Yamazawa K, Kagami M, Ogawa M, Horikawa R, Ogata T. 2008b. Placental hypoplasia in maternal uniparental disomy for chromosome 7. Am J Med Genet Part A 146A:514–516.

Yamazawa K, Nakabayashi K, Kagami M, Sato T, Saitoh S, Horikawa R, Hizuka N, Ogata T. 2010. Parthenogenetic chimaerism/mosaicism with a Silver-Russell syndrome-like phenotype. J Med Genet 47:782–785.

AUTHOR QUERY FORM

JOURNAL: AMERICAN JOURNAL OF MEDICAL GENETICS PART A
Article: ajma_34404

Dear Author,

During the copyediting of your paper, the following queries arose. Please respond to these by annotating your proofs with the necessary changes/additions.

- If you intend to annotate your proof electronically, please refer to the E-annotation guidelines.
- If you intend to annotate your proof by means of hard-copy mark-up, please refer to the proof mark-up symbols guidelines. If manually writing corrections on your proof and returning it as a scanned pdf via email, do not write too close to the edge of the paper. Please remember that illegible mark-ups may delay publication.

Whether you opt for hard-copy or electronic annotation of your proofs, we recommend that you provide additional clarification of answers to queries by entering your answers on the query sheet, in addition to the text mark-up.

Query No.	Query	Remark
Q1	Please check the grant sponsors.	
Q2	Please check the change made in the reference citation (Silver et al., 1953).	
Q3	Please give address information for this manufacturer: city, state (if applicable), and country.	
Q4	Please provide the volume number and page range.	

EJHG Open

European Journal of Human Genetics (2012), 1–5

www.nature.com/ejhg

ARTICLE

Relative frequency of underlying genetic causes for the development of UPD(14)pat-like phenotype

Masayo Kagami[1], Fumiko Kato[1], Keiko Matsubara[1], Tomoko Sato[1], Gen Nishimura[2] and Tsutomu Ogata*[,1,3]

Paternal uniparental disomy 14 (UPD(14)pat) results in a unique constellation of clinical features, and a similar phenotypic constellation is also caused by microdeletions involving the *DLK1-MEG3* intergenic differentially methylated region (IG-DMR) and/or the *MEG3*-DMR and by epimutations (hypermethylations) affecting the DMRs. However, relative frequency of such underlying genetic causes remains to be clarified, as well as that of underlying mechanisms of UPD(14)pat, that is, trisomy rescue (TR), gamete complementation (GC), monosomy rescue (MR), and post-fertilization mitotic error (PE). To examine this matter, we sequentially performed methylation analysis, microsatellite analysis, fluorescence *in situ* hybridization, and array-based comparative genomic hybridization in 26 patients with UPD(14)pat-like phenotype. Consequently, we identified UPD(14)pat in 17 patients (65.4%), microdeletions of different patterns in 5 patients (19.2%), and epimutations in 4 patients (15.4%). Furthermore, UPD(14)pat was found to be generated through TR or GC in 5 patients (29.4%), MR or PE in 11 patients (64.7%), and PE in 1 patient (5.9%). Advanced maternal age at childbirth (≥35 years) was predominantly observed in the MR/PE subtype. The results imply that the relative frequency of underlying genetic causes for the development of UPD(14)pat-like phenotype is different from that of other imprinting disorders, and that advanced maternal age at childbirth as a predisposing factor for the generation of nullisomic oocytes through non-disjunction at meiosis 1 may be involved in the development of MR-mediated UPD(14)pat.
European Journal of Human Genetics (2012) **0**, 000–000. doi:10.1038/ejhg.2012.26

Keywords: genetic cause; maternal age effect; monosomy rescue; UPD(14)pat subtype

INTRODUCTION

Human chromosome 14q32.2 carries a ~1.2 Mb imprinted region with the germline-derived primary *DLK1-MEG3* intergenic differentially methylated region (IG-DMR) and the post-fertilization-derived secondary *MEG3*-DMR, together with multiple imprinted genes.[1,2] Both DMRs are methylated after paternal transmission and unmethylated after maternal transmission in the body, whereas in the placenta the IG-DMR alone remains as a DMR and the *MEG3*-DMR is rather hypomethylated irrespective of the parental origin.[2,3] Furthermore, it has been shown that the unmethylated IG-DMR and *MEG3*-DMR of maternal origin function as the imprinting centers in the placenta and the body, respectively, and that the IG-DMR acts as an upstream regulator for the methylation pattern of the *MEG3*-DMR in the body but not in the placenta.[3]

As a result of the presence of the imprinted region, paternal uniparental disomy 14 (UPD(14)pat) (OMIM #608149) causes a unique constellation of body and placental phenotypes such as characteristic face, bell-shaped small thorax, abdominal wall defect, polyhydramnios, and placentomegaly.[2,4,5] Furthermore, consistent with the essential role of the DMRs in the imprinting regulation, microdeletions and epimutations affecting the IG-DMR or both DMRs of maternal origin result in UPD(14)pat-like phenotype in both the body and the placenta, whereas a microdeletion involving the maternally inherited *MEG3*-DMR alone leads to UPD(14)pat-like phenotype in the body, but not in the placenta.[2,3]

Of the three underlying genetic causes for UPD(14)pat-like phenotype (UPD(14)pat, microdeletions, and epimutations), UPD(14)pat is primarily generated by four mechanisms, that is, trisomy rescue (TR), gamete complementation (GC), monosomy rescue (MR), and post-fertilization mitotic error (PE).[6] TR refers to a condition in which chromosome 14 of maternal origin is lost from a zygote with trisomy 14 formed by fertilization between a disomic sperm and a normal oocyte. GC results from fertilization of a disomic sperm with a nullisomic oocyte. MR refers to a condition in which chromosome 14 of paternal origin is replicated in a zygote with monosomy 14 formed by fertilization between a normal sperm and a nullisomic oocyte. PE is an event after formation of a normal zygote. In this regard, a nullisomic oocyte specific to GC and MR is produced by non-disjunction at meiosis 1 (M1) or meiosis 2 (M2), and non-disjunction at M1 is known to increase with maternal age, probably because of a long-term (10–50 years) meiotic arrest at prophase 1.[7]

However, relative frequency of the genetic causes for UPD(14)pat-like phenotype remains to be determined, as well as that of underlying mechanisms for the generation of UPD(14)pat. Here, we report our data on this matter, and discuss the difference in the relative frequency

[1]Department of Molecular Endocrinology, National Research Institute for Child Health and Development, Tokyo, Japan; [2]Department of Radiology, Tokyo Metropolitan Children's Medical Center, Fuchu, Japan; [3]Department of Pediatrics, Hamamatsu University School of Medicine, Hamamatsu, Japan
*Correspondence: Professor T Ogata, Department of Pediatrics, Hamamatsu University School of Medicine, Hamamatsu 431-3192, Japan. Tel: +81 53 435 2310; Fax: +81 53 435 2312; E-mail: tomogata@hama-med.ac.jp
Received 23 May 2011; revised 10 November 2011; accepted 26 December 2011

among imprinted disorders and the possible maternal age effect on the relative frequency.

PATIENTS AND METHODS

Patients

This study comprised 26 patients with UPD(14)pat-like phenotype (9 male patients and 17 female patients) (Table 1). Of the 26 patients, 18 patients have been reported previously; they consisted of nine sporadic patients with full UPD(14)pat,[4,5] one sporadic patient with segmental UPD(14)pat,[4] the proband of sibling cases and four sporadic patients with different patterns of microdeletions involving the unmethylated DMRs of maternal origin,[2,3] and three patients with epimutations (hypermethylations) of the two normally unmethylated DMRs of maternal origin.[2] The remaining eight patients were new sporadic cases.

Phenotypic findings of the 26 patients are summarized in Supplementary Table 1; detailed clinical features of patients 6 and 16–25 are as described previously,[2–4] and those of the eight new patients 3, 5, 10–14, and 26 are shown in Supplementary Table 2, together with those of patients 1, 2, 4, 7–9, and 15 in whom detailed phenotypes were not described in the previous report.[5] All the 26 patients were identified shortly after birth because of the unique bell-shaped thorax with coat-hanger appearance of the ribs on roentgenograms obtained because of asphyxia. Subsequent clinical analysis revealed that 25 of the 26 patients exhibited both body and placental UPD(14)pat-like phenotype, whereas the remaining one previously reported patient (patient 22) manifested body, but not placental, UPD(14)pat-like phenotype.[3] The karyotype was found to be normal in 25 patients, although cytogenetic analysis was not performed in one previously reported patient who died of respiratory failure at 2 h of age (patient 6).[4] One patient (patient 15) was conceived by *in vitro* fertilization-embryo transfer.[5] This study was approved by the Institute Review Board Committee at the National Center for Child Health and Development, and performed after obtaining written informed consent.

Analysis of underlying genetic causes in patients with UPD(14)pat-like phenotype

We sequentially performed methylation analysis, microsatellite analysis, and fluorescence *in situ* hybridization (FISH), using leukocyte genomic DNA samples and lymphocyte metaphase spreads of all the 26 patients with UPD(14)pat-like phenotype. The detailed methods were as reported previously.[2,3] In brief, methylation analysis was performed for the IG-DMR (CG4 and CG6) and the *MEG3*-DMR (CG7 and the CTCF-biding sites C and D) by combined bisulfite restriction analysis and bisulfite sequencing. Microsatellite analysis was performed for multiple loci on chromosome 14, by determining the sizes of PCR products obtained with fluorescently labeled forward primers and unlabeled reverse primers. FISH analysis was carried out for the IG-DMR and the *MEG3*-DMR using 5104-bp and 5182-bp long PCR products, respectively, together with the RP11-566I2 probe for 14q12 utilized as an internal control.

In this study, furthermore, oligonucleotide array-based comparative genomic hybridization (CGH) was also performed for the imprinted region of non-UPD(14)pat patients, using a custom-build oligo-microarray containing 12 600 probes for 14q32.2–q32.3 encompassing the imprinted region and ~10 000 reference probes for other chromosomal region (4×180K format, Design ID 032112) (Agilent Technologies, Palo Alto, CA, USA). The procedure was as described in the manufacturer's instructions.

Analysis of subtypes in patients with UPD(14)pat

UPD(14)pat subtype was determined by microsatellite analysis.[8,9] In brief, heterodisomy for at least one locus was regarded as indicative of TR- or GC-mediated UPD(14)pat (TR/GC subtype), whereas isodisomy for all the informative microsatellite loci was interpreted as indicative of MR- or PE-mediated UPD(14)pat (MR/PE subtype) (for details, see Supplementary Figure S1). Here, while heterodisomy and isodisomy for a pericentromeric region in the TR/GC subtype imply a disomic sperm generation through M1

Table 1 Summary of patients examined in this study

Patient	*Genetic cause*	*UPD(14)pat subtype*	*Maternal age at childbirth (years)*	*Paternal age at childbirth (years)*	*Remark*	*Reference*
1	UPD(14)pat	TR/GC [M1]	31	35		5
2	UPD(14)pat	TR/GC [M1]	28	29		5
3	UPD(14)pat	TR/GC [M1]	29	38		This report
4	UPD(14)pat	TR/GC [M1]	36	41		5
5	UPD(14)pat	TR/GC [M2]	30	30		This report
6	UPD(14)pat	MR/PE	42	Unknown		4,5
7	UPD(14)pat	MR/PE	31	28		5
8	UPD(14)pat	MR/PE	32	33		5
9	UPD(14)pat	MR/PE	26	35		5
10	UPD(14)pat	MR/PE	38	38		This report
11	UPD(14)pat	MR/PE	26	32		This report
12	UPD(14)pat	MR/PE	41	36		This report
13	UPD(14)pat	MR/PE	30	28		This report
14	UPD(14)pat	MR/PE	39	34		This report
15	UPD(14)pat	MR/PE	42	37	Born after IVF-ET	5
16	UPD(14)pat	MR/PE	36	36		4,5
17	UPD(14)pat-seg.	PE	27	24	Segmental isodisomy	4,5
18	Microdeletion		31	34		2
19	Microdeletion		33	36		2
20	Microdeletion		28	27		2
21	Microdeletion		27	37	IG-DMR alone	3
22	Microdeletion		25	25	*MEG3*-DMR alone	3
23	Epimutation		35	36		2
24	Epimutation		28	26		2
25	Epimutation		27	30		2
26	Epimutation		33	33		This report

Abbreviation: IVF-ET, *in vivo* fertilization-embryo transfer using parental gametes.
The microdeletions in patients 18–22 are different in size.

and M2 non-disjunction respectively,[9] such discrimination between M1 and M2 non-disjunctions is impossible for the development of a nullisomic oocyte. Furthermore, it is usually impossible to discriminate between TR and GC, although the presence of trisomic cells is specific to TR. Similarly, it is also usually impossible to discriminate between MR and PE, although identification of segmental isodisomy or mosaicism is unique to PE (PE subtype).

Analysis of parental ages

We examined parental ages at childbirth in patients of different underlying causes and different UPD(14)pat subtypes. Statistical significance of the relative frequency was examined by the Fisher's exact probability test, and that of the median age by the Mann–Whitney's *U*-test. $P<0.05$ was considered significant.

RESULTS

Analysis of underlying causes in patients with UPD(14)pat-like phenotype

For the eight new sporadic patients, methylation analysis invariably revealed hypermethylation of both DMRs, and microsatellite analysis showed UPD(14)pat in seven patients and biparentally inherited homologs of chromosome 14 in the remaining one patient (patient 26). FISH analysis for patient 26 identified two signals for the two DMRs, and subsequently performed array CGH analysis showed no evidence for genomic rearrangements (Supplementary Figure S2). Thus, patient 26 was assessed to have an epimutation affecting the two DMRs. Furthermore, the results of array CGH analysis confirmed the presence of microdeletions in patients 18–21 and the absence of a discernible microdeletion in patients 23–25 (Supplementary Figure S2) (array CGH analysis was not performed in patient 22 with a 4303-bp microdeletion[3] because of the lack of DNA sample available). Thus, together with our previous data, all the 26 patients with UPD(14)pat-like phenotype had genetic alteration involving the imprinted region on chromosome14q32.2.

Consequently, the 26 patients with UPD(14)pat-like phenotype were classified as follows: (1) 16 sporadic patients with full UPD(14)pat and 1 sporadic patient with segmental UPD(14)pat (UPD(14)pat group); (2) the proband of the sibling cases and two sporadic patients with different patterns of microdeletions involving the two DMRs, one sporadic patient with a microdeletion involving the IG-DMR alone in whom the *MEG3*-DMR was epimutated, and one patient with a microdeletion involving the *MEG3*-DMR alone (deletion group); and (3) four patients with epimutations (hypermethylations) of both DMRs (epimutation group) (Figure 1 and Table 1).

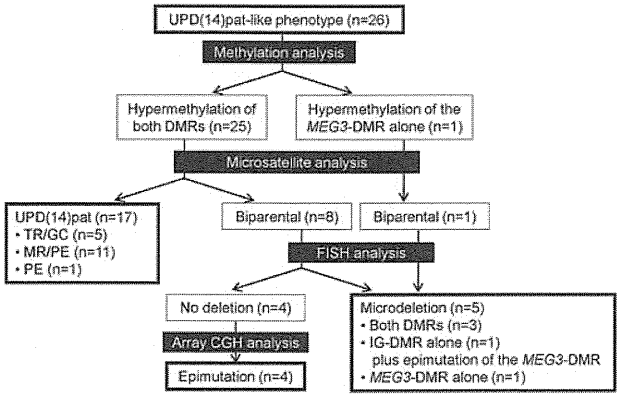

Figure 1 Classification of 26 patients with UPD(14)pat-like phenotype.

Analysis of subtypes in patients with UPD(14)pat

Heterozygosity for at least one locus indicative of TR/GC subtype was identified in five patients (patients 1–5), and the disomic pattern of pericentromeric region indicated M1 non-disjunction in patients 1–4 and M2 non-disjunction in patient 5. Full isodisomy consistent with MR/PE subtype was detected in 11 patients (patients 6–16), and segmental isodisomy unique to PE subtype was revealed in 1 patient (patient 17) (Table 1, Figure 1, and Supplementary Figure S3).

Analysis of parental ages

The distribution of parental ages at childbirth is shown in Figure 2. The advanced maternal age at childbirth (≥35 years) was predominantly observed in the MR/PE subtype of UPD(14)pat. Furthermore, while the relative frequency of aged mothers (≥35 years) did not show a significant difference between the MR/PE subtype of UPD(14)pat (6/11) and (i) other subtypes of UPD(14)pat (1/6) (P=0.159), (ii) deletion group (0/5) (P=0.057), and (iii) epimutation group (1/4) (P=0.338), it was significantly different between the MR/PE subtype and the sum of other subtypes of UPD(14)pat, deletion group, and epimutation group (2/15) (P=0.034). Similarly, while the median maternal age did not show a significant difference between the MR/PE subtype of UPD(14)pat (36 years) *vs* (i) other subtypes of UPD(14)pat (29.5 years) (P=0.118), (ii) deletion type (28 years) (P=0.088), and (iii) epimutation type (30.5 years) (P=0.295), it was significantly different between the MR/PE subtype of UPD(14)pat and the sum of other subtypes of UPD(14)pat, deletion group, and epimutation group (29 years) (P=0.045).

The paternal ages were similar irrespective of the genetic causes and the UPD(14)pat subtypes. In addition, the median paternal age was comparable between the TR/GC subtype of UPD(14)pat that postulates the production of a disomic sperm (35.0 years) and the sum of other subtypes of UPD(14)pat, deletion group, and epimutation group that assumes the production of a normal sperm (33.5 years) (P=0.322).

DISCUSSION

This study revealed that the UPD(14)pat-like phenotype was caused by UPD(14)pat in 65.4% of patients, by microdeletions in 19.2% of patients, and by epimutations in 15.4% of patients. Although the relative frequency of underlying genetic factors for the development of UPD(14)pat-like phenotype has been reported previously,[10] most data are derived from our previous publications. Thus, the present results are regarded as the updated and extended data on the relative frequency. For the relative frequency, it is notable that 25 of the 26 patients were confirmed to have normal karyotype, although chromosome analysis was not performed in patient 6. Thus, while Robertsonian translocations involving chromosome 14 is known to be a

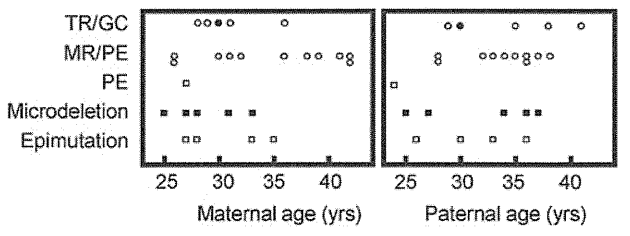

Figure 2 The distribution of parental ages at childbirth according to the underlying genetic causes for the development of UPD(14)pat-like phenotype and UPD(14)pat subtypes. Of the five plots for the TR/GC subtype, open and black circles indicate the TR/GC subtype due to non-disjunction at paternal M1 and M2, respectively.